Temporal and spatial significance of volcanic particles in sand(stone): implications for provenance and palaeotectonic reconstructions

Published Version:
Salvatore Critelli, S.C. (2022). Temporal and spatial significance of volcanic particles in sand(stone): implications for provenance and palaeotectonic reconstructions. Londra : Geological Society of London [10.1144/SP520-2022-99].

Availability:
This version is available at: https://hdl.handle.net/11585/904199 since: 2022-11-19

Published:

DOI: http://doi.org/10.1144/SP520-2022-99

Accepted Manuscript

Geological Society, London, Special Publications

Temporal and spatial significance of volcanic particles in sand (stone): implications for provenance and paleotectonic reconstructions

Salvatore Critelli, Sara Criniti, Raymond V. Ingersoll & William Cavazza

DOI: https://doi.org/10.1144/SP520-2022-99

To access the most recent version of this article, please click the DOI URL in the line above. When citing this article please include the above DOI.

Received 29 March 2022
Revised 22 June 2022
Accepted 6 July 2022

Temporal and spatial significance of volcanic particles in sand (stone): implications for provenance and paleotectonic reconstructions

Salvatore Critelli [1*], Sara Criniti [1], Raymond V. Ingersoll [2] and William Cavazza [3]

[1] Department of Biology, Ecology and Earth Sciences, University of Calabria, 87036 Rende (CS), Italy

[2] Department of Earth, Planetary, and Space Sciences, University of California, Los Angeles, California, 90095-1567, U.S.A.

[3] Department of Biological, Geological and Environmental Sciences, University of Bologna, Piazza Porta San Donato 1, 40126 Bologna, Italy

* correspondence: salvatore.critelli@unical.it

Abstract: Volcanic particles have particular geodynamic significance. Despite abundant datasets on volcanic-derived sand(stone), the distinction between spatial and temporal distribution of volcanic particles within the sedimentary record is poorly documented. One of the most intricate tasks in optical analysis of volcaniclastic sand(stone) is the distinction of grains eroded from ancient volcanic rocks (paleovolcanic, noncoeval grains) from grains generated by active volcanism during sedimentation (neovolcanic coeval grains). Petrologic methods are useful for deciphering temporal significance of volcanic particles in detail between paleovolcanic and neovolcanic, and for active volcanism to decipher syneruptive versus posteruptive processes during deposition in sedimentary basins close to volcanoes. Sedimentary processes during syneruptive, intereruptive and posteruptive phases are well described in continental environments in terms of changing sedimentary facies, for example, the architecture (from body scale to stratigraphic scale), width/depth ratios of paleochannels, palesols and composition of fluvial-channel deposits, whereas they are less documented in deep-marine environments. Examples of volcaniclastic sedimentation derived from both paleovolcanic and neovolcanic sources are found in diverse geotectonic settings.

Keywords: Volcaniclastic sedimentation; Neovolcanic; Paleovolcanic; Plate settings.

Introduction

Quantitative clastic petrology is a powerful tool for interpreting provenance of detrital signatures, providing key insights regarding processes occurring in terrestrial and marine environments and for reconstructing the tectonic and paleogeographic evolution of mountain belts and associated sedimentary basins (e.g. Dickinson, 1970a, 1985; Dickinson and Suczek, 1979; Valloni, 1985, Zuffa, 1987; Ingersoll, 1990; Garzanti *et al*., 2007; Critelli and Criniti, 2021). In the puzzle of detrital budgets in sand(stone), lithic fragments contain crucial information on fabrics and paragenesis of source rocks. Characteristics of grain types in sand(stone) are crucial for solving key questions related to source-to-sink quantitative analysis. One of the most intriguing questions in source-to-sink analysis is definition of the temporal and spatial relationships between the generation of clastic particles in their source areas and accumulation basins (e.g. Zuffa, 1980, 1985, 1987; Ingersoll *et al*., 1984; Critelli and Ingersoll, 1995; Critelli *et al*., 2007). Among all the particle types, volcanic grains in sand(stone) illustrate how deciphering of spatial and temporal provenance may be useful for detailed paleogeographic and paleotectonic reconstructions (e.g., Zuffa, 1985, 1987). Volcanic debris can derive from (i) dismantling by chemical/physical weathering and transport of ancient volcanic rocks (paleovolcanic grains) or (ii) generated by active volcanism during sedimentation (neovolcanic grains) (e.g., Zuffa, 1985, 1987). Textural attributes may directly reflect the contrasting compositional signature of volcanic eruptions (Marsaglia and Ingersoll, 1992; Marsaglia, 1993; Critelli *et al*., 2002; Affolter and Ingersoll, 2019; Le Pera and Morrone, 2020; Le Pera *et al*., 2021).

Our method of petrographic modal analysis is designed to quantify the textural attributes of pyroclastic and epiclastic debris that reflect eruption style, in addition to those that relate to magma composition. The modal analysis of textures makes use of descriptive classes of shard morphology commonly referred to by volcanologists (e.g., Heiken and Wohletz, 1985) in SEM (scanning electron microscope) studies and quantified in modal analysis of lithified rocks by De Rosa (1999). The modal analysis of detrital magmatic components to determine source-rock composition was developed by sedimentary petrologists (e.g. Gazzi, 1966;

Dickinson, 1970a; Zuffa, 1980, 1985, 1987; Ingersoll and Cavazza, 1991; Marsaglia, 1992, 1993; Critelli and Ingersoll, 1995; Marsaglia and Devaney, 1995; Critelli *et al*., 2002) to help fingerprint mafic, intermediate and felsic components, and their relative proportions in volcaniclastic sediments. To quantify these parameters in combination provides a unique approach to interpreting the provenance of volcaniclastic sediments deposited in marine settings, where reworking and mixing can be common processes.

This paper utilizes petrological methods to discriminate neovolcanic and paleovolcanic detritus, and particularly to decipher syneruptive, intereruptive and posteruptive processes and their signatures during sedimentary basin evolution. We explain our classification method and relevant features of volcanic lithic grains, which allows us to retrieve significant information during point counting of volcaniclastic sand and sandstone, and ensure data reproducibility.

Methods

In order to distinguish paleovolcanic and neovolcanic contributions (e.g. Critelli and Ingersoll, 1995; Critelli *et al*., 2002), we use a point-count procedure for volcaniclastic sand(stone) that quantifies the diverse information that volcanic detritus can reveal in optical analysis **(Fig. 1)**. Table 1 contains standard point-count categories modified for volcanic detritus; Table 2 distinguishes paleovolcanic from neovolcanic contributions. Interstices in volcaniclastic sandstones may have fine-grained volcanogenic matrix consisting of fine ash. Authigenic minerals may include clay, dolomite, coliform silica, zeolites, authigenic albite, phyllosilicate and quartz.

Classification of volcanic grains

Volcanic grains are subdivided into four main groups (lathwork, microlitic, felsitic and vitric) **(Fig. 2)**; this operational classification proposed by Dickinson (1970a) focuses on those volcanic textures that are particularly useful in the study of volcanic arenite.

Vitric or Vitrophyric texture

Vitric or vitrophyric grains and shards are glass or altered glass, which may include phyllosilicates, zeolites, feldspars, silica minerals or combinations of these in microcrystalline aggregates **(Fig. 3)**. These textures are especially common in silicic volcanic rocks, even if they can also occur in more femic volcanic rocks as palagonitic sideromelane glass of basalts (Fig. 3A, B, C), or as black tachylitic glass in andesite. Vitric volcanic lithic fragments (Lvv) are defined as pumice or scoria and glass shards, but also include partially to wholly altered glass (Dickinson, 1970a; Ingersoll and Cavazza, 1991; Marsaglia, 1992). Every sample has either blocky shards (of hydroclastic origin) (Fig. 3D) or scoria fragments (of explosive magmatic origin); some of the scoria fragments are blocky, indicating phreatomagmatic eruptions (e.g., Fisher and Schmincke, 1984; Heiken and Wohletz, 1985; McPhie *et al*., 1993; White and Houghton, 2006; Sohn et al., 2008).

Textural attributes of volcanic glass fragments can indicate the style of active volcanism during sedimentation, such as spatial occurrence of eruptions, (i) colorless glass, both blocky shards and bubble-wall shards, Y-shaped glass (Fig. Fig. 3E, F) and pumice fragments are closely related to subaerial explosive mainly silicic volcanism; (ii) black glass or tachylitic glass is closely related to subaerial volcanism, both explosive and nonexplosive mainly intermediate (andesitic) silicic-volcanic eruptions; (iii) brown glass is closely related to subaerial or subaqueous volcanism, both explosive and nonexplosive mainly intermediate to mafic-volcanic (basaltic to andesitic) eruptions (iv) orange glass (quenched glass and palagonitic sideromelane glass) is closely related to dominantly subaqueous mafic-volcanic (basaltic to basaltic andesite) eruptions (Fig. 3A, B, C) (e.g. Heiken and Wohletz, 1985; Marsaglia, 1992; Critelli and Ingersoll, 1995; Critelli *et al*., 2002).

Microlitic texture

Microlitic volcanic lithic fragments (Lvmi) are defined as fragments that contain variable amounts of microlites of plagioclase or ferromagnesian minerals that are visible at high magnification and are <0.0625 mm long (Dickinson, 1970a). Microlitic texture is typical of andesites, but it also commonly occurs in basalts and basaltic andesites. See Affolter and Ingersoll (2019) for discussion of correlations between volcanic textures and compositions.

Plagioclase and ferromagnesian microlites usually occur in dominantly black, brown or orange vitric groundmass. The microlitic texture is similar to intergranular and hyalophitic textures in basalt lava. Felsic microlitic fragments consist of pumice fragments with microlites of plagioclase **(Fig. 4)**.

Lathwork texture

Lathwork volcanic lithic fragments (Lvl), as first defined by Dickinson (1970a), have greater-than-0.0625 mm phenocrysts in a groundmass of glass or devitrified glass (Fig. 3, A and B). This texture is characteristic of basaltic and basaltic andesite lavas and pyroclasts. Phenocrystic phases of basalt lava flows include plagioclase (dominantly labradorite and bytownite-labradorite), clinopyroxene as diopside, other pyroxenes, and rare olivine and iron-titanium oxides. The glassy groundmass is black, brown or orange, and may be microlitic. According to the textural subdivision of volcanic rocks of Williams *et al*. (1954), the basalts show intersertal, intergranular, and hyalophitic textures **(Fig. 5)**.

Felsitic textures

Phenocrystic phases in dacite and rhyolite include plagioclase (zoned from labradorite/andesine to oligoclase/albite), green hornblende, quartz, biotite and potassium feldspar. Groundmass minerals usually include plagioclase, quartz, hornblende and magnetite. The dominant groundmass texture is felsitic granular, consisting of an anhedral microcrystalline mosaic composed mainly of quartz and feldspar with uniform, very fine grain size. Hyalopilitic texture, in which colorless glass occupies the minute interspaces between randomly oriented microlites of plagioclase, is also common. In some cases, the glass is largely recrystallized (granular texture) (Affolter and Ingersoll, 2019). Vitrophyric texture in which phenocrysts lie in a matrix of glass (with or without minor alteration and/or devitrification of the glass) also occurs in felsitic textures.

Felsitic volcanic lithic fragments (Lvf) include two types, seriate and granular (Dickinson, 1970a; Ingersoll and Cavazza, 1991).

Felsitic seriate texture is an anisometric mosaic, with a wide range of crystal sizes and shapes, composed mainly of feldspar, quartz and/or mafic minerals. Usually, felsitic seriate grains include abundant plagioclase, hornblende and biotite phenocrysts in a vitric or microcrystalline groundmass, and represent mainly silicic-volcanic rocks, either lava or tuff, especially high-K varieties **(Fig. 6A, B, C)**. This texture includes all volcanic grains that do not fit any of the other categories. Felsitic seriate texture is typical of dacite and andesite (Ingersoll and Cavazza, 1991).

Felsitic granular texture consists of anhedral microcrystalline mosaics, with uniform very fine grain size, composed mainly of quartz and feldspar with rare mafic minerals, and represents mainly silicic-volcanic rocks, either lava or tuff **(Fig. 6D, E, F)**. Vitric grains may grade into granular grains through devitrification. Felsitic granular texture is typical of rhyolite, rhyodacite and dacite (Ingersoll and Cavazza, 1991).

Applications and Implications

Volcanic detritus in sandstone is useful working on problems of sediment provenance. As an example, the guidelines for petrographic recognition of paleovolcanic and neovolcanic detritus provide a conceptual and methodological tool kit to help sort out syneruptive, intereruptive and posteruptive sedimentation. A first step of temporal recognition between paleo- versus neovolcanic particles may be useful for better understanding the geological setting during deposition (coeval or neovolcanic grains). A more sophisticated approach is to solve coeval source-to-sink problems, distinguishing all time phases of volcanism and related sedimentation in associated sedimentary basins. During syneruptive sedimentation, pure volcanolithic sand(stone) is interbedded with primary volcanic rocks and reflects mostly homogeneous volcanic detritus. During intereruptive sedimentation, impure volcanolithic sand(stone) is deposited in response to different eruptive phases and is mixed with nonvolcanic detritus. During posteruptive sedimentation, neovolcanic detritus progressively decreases and is largely mixed with nonvolcanic detritus (e.g., Smith, 1991; Critelli and Ingersoll, 1995; D'Elia *et al*., 2018; Di Capua. and Groppelli, 2018; Di Capua and Scasso, 2020).

Syneruptive volcaniclastic petrofacies

Mafic syneruptive volcaniclastic suites

Mafic syneruptive volcaniclastic sand(stone) suites consist dominantly of volcanic lithic fragments, largely exhibiting lathwork and microlitic textures and subordinate vitric textures. Single crystals of plagioclase, clinopyroxene and other monocrystalline grains are less abundant (e.g. Marsaglia, 1993; Critelli and Ingersoll, 1995; Critelli *et al*., 2002; Affolter and Ingersoll, 2019; Jafarzadeh *et al*., 2022). Basalt clasts vary from dense nonvesicular types to highly vesicular scoria fragments, the latter having either blocky shards or fragments of scoria, resulting from nonexplosive to mildly explosive thermal contraction and shattering of glass in phreatomagmatic eruptions, typical of deep-water volcanism (e.g. Heiken and Wohletz, 1985).

Intermediate syneruptive volcaniclastic suites

Intermediate syneruptive volcaniclastic sand(stone) suites consist dominantly of volcanic lithic fragments and minor plagioclase and quartz, largely exhibiting microlitic and felsitic seriate textures and subordinately vitric textures. Single crystals of plagioclase, hornblende, pyroxene and other monocrystalline grains are present (e.g. Packer and Ingersoll, 1986; Marsaglia and Ingersoll, 1992; Marsaglia *et al*., 1992; Smith and Lotosky, 1995). Andesitic ash consists of mixtures of vitric, crystal and lithic components. Glass is brownish, black to colorless (Heiken and Wohletz, 1985). Clasts vary from low vesicularity to medium-vesicular or blocky fragments (e.g. Heiken and Wohletz, 1985); poorly vesicular tephra lacking distinctive pumiceous and bubble-wall textures of more silicic pyroclasts also occur (Fisher and Schmincke, 1984; Heiken and Wohletz, 1985). Fresh green hornblende is useful as a measure of pyroclastic input (e.g. Smith and Lotosky, 1995). Crystal-rich andesite sand often results from eruptive processes that physically fractionate particles by density and grain size (Smith and Lotosky, 1995).

Felsic *syneruptive volcaniclastic suites*

Felsic syneruptive volcaniclastic sand(stone) suites consist dominantly of felsitic granular lithic fragments, with lesser vitric lithic fragments. Single crystals which are usually more abundant in the felsic sand suites than in the mafic sand suites, consist of plagioclase, quartz, hornblende and K-feldspar. When the ratio of unaltered green hornblende to total hornblende is high (0.9–1.0), felsic volcaniclastic sand(stone) suites are likely syneruptive facies, as defined by Erskine and Smith (1993) and Smith and Lotosky (1995). Furthermore, a pyroclastic source is indicated by this ratio because unaltered green hornblende is not found in lava flows (Smith and Lotosky, 1995). Some syneruptive felsic sand(stone) suites are composed largely of glass. Glass has bubble-wall shards or pumice, or dominantly platy shards and bubble-wall shards. Abundant platy shards indicate granulation by contact of magma with water (Heiken and Wohletz, 1985). The contribution of abundant pumice and bubble-wall shards and absence of platy or blocky shards indicate explosive magmatic eruptions in the absence of external water (e.g. Critelli *et al*., 2002).

Tectonic implications

Most volcaniclastic sand(stone) produced in both young and ancient volcanic provinces is associated with magmatic arcs (e.g., Dickinson and Suczek 1979; Dickinson, 1982, 1985; Maynard *et al*. 1982; Cawood 1983; Critelli et al., 1990; 2002; Marsaglia and Ingersoll 1992; Critelli, 1993; Marsaglia *et al*., 2016; Morrone *et al*. 2017, 2020; Le Pera *et al*., 2021), but is also present in continental rifts (e.g., Ingersoll 1990; Ingersoll *et al*. 1993), as well as in orogenic (e.g., Critelli and Le Pera, 1995, 1998; Garzanti *et al*., 1996; Caracciolo *et al*., 2011, 2012, 2015, 2016; Critelli *et al*., 2011, 2017; Cavazza *et al*., 2013; Critelli, 2018; Critelli and Criniti, 2021) and strike-slip settings (e.g. Critelli and Ingersoll, 1995; Critelli *et al*., 1997) **(Fig. 7)**. Even though volcanic lithic fragments are chemically reactive and prone to compaction, they are still useful in provenance studies because textures can be preserved and identified even after significant alteration (e.g., Affolter and Ingersoll, 2019 and bibliography therein).

Magmatic-arc systems. - Modern and ancient examples of arc-trench systems and related sedimentary basins are the most obvious tectonic settings in which volcanism and sedimentation are intimately related. Trench-fill successions, and forearc, intra-arc and backarc basins are the sites of preferential accumulation of volcaniclastic sand(stone). Modern arc-trench systems, particularly in the Circum-Pacific region, have been largely used to document the types and occurrence of volcanic particles and dispersal pathways within magmatic arcs and adjacent sedimentary basins (e.g. Marsaglia and Ingersoll, 1992; Marsaglia, 1991; Critelli *et al*., 2002; Malekzadeh *et al*., 2020). Other key modern examples of volcaniclastic sand are found in the eastern Tyrrhenian Sea (e.g. Morrone *et al*., 2017, 2020, 2022; Le Pera and Morrone, 2020) and Aegean Sea forearc (Saccani, 1987) and back-arc basins.

Ancient sedimentary strata related to arc-trench systems have been milestones for determining plate-tectonic settings (e.g. Dickinson, 1970b; 1973; 1976; Ingersoll, 2012). Sandstone strata in ancient sedimentary basins of arc-trench systems record the evolution of convergent margins and have been used to reconstruct the evolution of source-to-sink systems. Because several arc-trench basins (e.g. backarc and intra/interarc) have low-to-medium preservation potential (e.g. Ingersoll, 2012), ancient examples are rare (e.g. Packer and Ingersoll, 1986; Marsaglia and Devaney, 1995; Critelli *et al*., 2002; Marsaglia et *al*., 2016; Malekzadeh *et al*., 2020; Jafarzadeh *et al*., 2022). Magmatic-arc-related basins include all kinds of calc-alkaline coeval volcaniclastic strata, in which observations became the basis for the subdivision of volcanic lithic fragments based on textural attributes (e.g., lathwork, microlitic, felsitic and vitric) (e.g., Dickinson, 1970a; Marsaglia, 1991; Marsaglia and Ingersoll, 1992).

Orogenic Systems. - In suture belts, including remnant ocean basins and proforeland settings, volcaniclastic sand(stone) and tuff are minor but can be key marker beds. Typical sand(stone) suites are quartzolithic and quartzofeldspathic (recycled orogenic provenance suites) (Dickinson and Suczek, 1979; Dickinson, 1985; Critelli and Criniti, 2021). The Circum-Mediterranean Region (e.g. Critelli, 1993, 2018; Critelli and Le Pera, 1994, 1995, 1998; Garzanti *et al*., 2007; Critelli and Criniti, 2021) and the southern continental margin Eurasia have several examples of volcaniclastic sand(stone) interbedded with quartzolithic suites, in both remnant ocean basins and foreland basins (e.g. Critelli *et al*., 1990; Caracciolo *et al*., 2011, 2015, 2016; Cavazza *et al*., 2013; Malekzadeh *et al*., 2020; Di Capua et al., 2021a, 2021b; Jafarzadeh *et al*., 2022).

Transform Settings. - Structural and stratigraphic development of strike-slip basins may result from crustal extension with thermal subsidence (transtensional) or flexural loading due to compression and sedimentary loading (transpressional) (Ingersoll, 2012). In all tectonic stages of evolving strike-slip basins, particularly when crustal extension occurs abruptly, coeval volcanism may produce primary erupted material interbedded with sedimentary strata. Volcaniclastic sedimentation may happen during all phases of volcanism activity and from subaerial to subaqueous. The Los Angeles basin area contains widely exposed and well studied strike-slip basins illustrating well documented relations between active volcanism and turbidite sedimentation during the Miocene (e.g. Critelli and Ingersoll, 1995).

Continental rifts. - Continental rifts may experience two life paths: “successful” rifting that evolves into seafloor spreading to form nascent ocean basins (Leeder, 1995; Ingersoll, 2012), which then evolve into active ocean basins with paired intraplate margins, or “failed” rifting, which does not evolve into nascent ocean basins, instead producing fossil rifts, commonly overlain by intracratonic basins (Sengor, 1995; Ingersoll, 2012). As continental lithosphere is stretched and thinned, mantle asthenosphere eventually rises toward the surface. During continental rifting, continual interaction between sedimentary and volcanic activity is common. The Cenozoic continental deposits of north-central New Mexico and southern Colorado record major tectono-magmatic events; resulting sand(stone) has provided critical constraints for reconstruction of ancient eruptive and dispersal systems, as well as constraining timing of tectonic events (e.g. Ingersoll, 1990, 2001; Ingersoll and Cavazza, 1991).

Rifted continental margins. - During the transition from continental rifting to the creation of nascent ocean basins, volcanism evolves from the bimodal compositions typical of continental extension to the creation of basaltic oceanic crust through the process of seafloor spreading (Dickinson, 1976; Garzanti *et al*., 2001; Ingersoll, 2012). Volcaniclastic deposits are commonly interbedded with continental redbeds and evaporite series in many fossil-rift successions, preserved following continental breakup. Nice examples occur in the Cenozoic of modern East Africa and the Red Sea (Garzanti et al., 2001). Widespread volcanics and volcaniclastic sandstone were deposited during late Carboniferous-to-Triassic break up of Pangaea (Critelli, 2018; Elter *et al*., 2020). These volcaniclastic sandstones deposited in fluvial to lacustrine environments are interbedded with ignimbrites, lava flows and ash beds, ranging from andesite to rhyolite in several locations in continental Europe and Sardinia.

Conclusions

This contribution illustrates the usefulness of volcaniclastic sand/sandstone suites in the reconstruction of ancient eruptive, dispersal and depositional systems. Traditionally, volcanic components in sand(stone) have been interpreted as responses to active volcanism or dismantling of remnant volcanic edifices. Less attention has been given to interpretation of volcanic detrital signals in the stratigraphic evolution of sedimentary basins to reveal the close relations of volcanogenic processes and transfer of detritus into basins (e.g. Cas and Wright, 1987; Fisher and Smith, 1991). Volcanic particles in the sedimentary budget can reveal detailed information in source-to-sink analysis in terms of the more specific processes that generate pyroclastic, hydroclastic, autoclastic and epiclastic volcanic particles.

The close relationships between erupted materials and characteristics of neovolcanic grains within the framework of eruption-related sand(stone) may reveal provenance signatures that record volcanic activity at a detailed scale. Neovolcanic detritus is dominant in syneruptive, intereruptive and immediately post-eruptive sandstone suites; in contrast, it is abruptly reduced in post-eruptive sand(stone) suites.

The nature of textural attributes of volcanic glass fragments can also indicate characteristics of active volcanism during sedimentation: (i) colorless glass, including blocky shards, bubble-wall shards and pumice fragments is closely related to subaerial explosive volcanism, mainly silicic-volcanic eruptions; (ii) black glass or tachylitic glass is closely related to subaerial volcanism both explosive or as lava of mainly intermediate (andesitic) silicic-volcanic eruptions; (iii) brown glass is closely related to subaerial or subaqueous volcanism, both explosive or as lava of mainly intermediate to mafic-volcanic (basaltic to andesitic) eruptions; and (iv) orange glass quenched glass and palagonitic sideromelane glass are closely related to dominantly subaqueous volcanism of mafic-volcanic (basaltic to basaltic andesite) eruptions.

As a corollary, optical methods can be used to determine compositional, spatial, temporal and textural characteristics of volcanic grains in sedimentary basins. This approach can be very useful for deciphering the evolutionary record of tectonics and sedimentation worldwide in time and space.

Acknowledgments

This chapter was supported by the “Laboratory of Geodynamics, Geo-Paleobiology and Earth Surface Processes” of the Department of Biology, Ecology and Earth Sciences at the University of Calabria. This research was funded by MUR (Ministry of University and Research), MUR-PRIN Project 2006.04.8397 “The Cenozoic clastic sedimentation within the circum-Mediterranean orogenic belts: implications for palaeogeographic and palaeotectonic evolution”, the 2010-2012 MUR-PRIN Project The Thrace sedimentary basin (Eocene-Quaternary; Turkey, Greece, Bulgaria): stratigraphic depositional architecture and sediment dispersal pathway within postorogenic basins”, and the University of Calabria MUR-ex60% Projects (Relationships between Tectonic Accretion, Volcanism and Clastic Sedimentation within the Circum-Mediterranean Orogenic Belts, 2006-2018; and "Palaeotectonics and palaeogeography of the Supercontinent Pangaea from Late Carboniferous to Triassic" support to S. Critelli). Sara Criniti was supported by the PhD Course in “Science and Engineering of Environment, Building and Energy” at the University of Calabria. The authors thank A. Di Capua and E. Le Pera for inviting us to submit this chapter, and A. Di Capua and an anonymous reviewer,for their helpful suggestions.

References

Affolter, M.D. and Ingersoll, R.V. 2019. Quantitative analysis of volcanic lithic fragments. *Journal of Sedimentary Research*, **89**, 479-486.

Caracciolo L., Critelli S., Innocenti F., Kolios N. and Manetti P. 2011, Unravelling provenance from Eocene-Oligocene sandstones of the Thrace Basin, North-east Greece. *Sedimentology*, **58**, 1988-2011.

Caracciolo L., Von Eynatten H., Tolosana-Delgado R., Critelli S., Manetti P. and Marchev P. 2012. Petrological, geochemical, and statistical analysis of Eocene-Oligocene sandstones of the Western Thrace Basin, Greece and Bulgaria. *Journal of Sedimentary Research*, **82**, 482-498.

Caracciolo L., Critelli S., Cavazza W., Meinhold G., von Eynatten H. and Manetti P. 2015. The Rhodope Zone as a primary sediment source of the southern Thrace basin (NE Greece and NW Turkey): Evidences from detrital heavy minerals and implications for central-eastern Mediterranean paleogeography. *International Journal of Earth Sciences*, **104**, 815-832.

Caracciolo L., Orlando A., Marchev P., Critelli S., Manetti P., Raycheva R. and Riley D. 2016. Provenance of Tertiary volcanoclastic sediment in NW Thrace (Bulgaria): Evidence from detrital amphibole and pyroxene geochemistry. *Sedimentary Geology*, **336**, 120-137.

Cas, R.A.F. and Wright, J.V. 1987. *Volcanic Successions, Modern and Ancient*. Allen and Unwin, London, 528 p.

Cavazza W., Caracciolo L., Critelli S., D'Atri A. and Zuffa G.G. 2013. Petrostratigraphic evolution of the Thrace Basin (Bulgaria, Greece, Turkey) within the context of Eocene-Oligocene post-collisional evolution of the Vardar-Izmir-Ankara suture zone. *Geodinamica Acta*, **26**, 12-26.

Cawood, P.A. 1983. Modal composition and detrital clinopyroxene geochemistry of lithic sandstones from the New England Fold Belt (east Australia): a Paleozoic forearc terrane. *Geological Society of America Bulletin*, **9**4, 1199–1214.

Critelli, S. 1993. Sandstone detrital modes in the Paleogene Liguride Complex, accretionary wedge of the Southern Apennines (Italy). *Journal of Sedimentary Petrology*, **63**, 464-476.

Critelli, S. 2018. Provenance of Mesozoic to Cenozoic Circum-Mediterranean sandstones in relation to tectonic setting. *Earth-Science Reviews*, **185**, 624-648.

Critelli, S. and Criniti, S. 2021. Sandstone Petrology and Provenance in Fold Thrust Belt and Foreland Basin System. In: Ali Ismail Al-Juboury (ed.) *Sedimentary Petrology - Implications in Petroleum Industry*. Intech Open Access Publisher, Janeza Trdine 9, Rijeka, Croatia, p. 1-15.[DOI: 10.5772/intechopen.96985].

Critelli S. and Ingersoll, R.V. 1995, Interpretation of neovolcanic versus palaeovolcanic sand grains: an example from Miocene deep-marine sandstone of the Topanga Group (Southern California). *Sedimentology*, **42**, 783-804.

Critelli, S. and Le Pera, E. 1994. Detrital modes and Provenance of Miocene sandstones and Modern sands of the Southern Apennines thrust-top basins (Italy). *Journal of Sedimentary Research*, **A64**, 824-835.

Critelli, S. and Le Pera, E. 1995. Tectonic evolution of the Southern Apennines thrust-belt (Italy) as reflected in modal compositions of Cenozoic sandstone. *The Journal of Geology*, **103**, 95-105.

Critelli, S. and Le Pera, E. 1998. Post-Oligocene sediment dispersal systems and unroofing history of the Calabrian Microplate, Italy. *International Geology Review*, **48**, 609-637.

Critelli, S., De Rosa, R. and Platt, J.P. 1990. Sandstone detrital modes in the Makran accretionary wedge, southwest Pakistan: Implications for tectonic setting and long-distance turbidite transportation. *Sedimentary Geology*, **68**, 241-260.

Critelli, S., Le Pera, E. and Ingersoll, R.V. 1997. The effects of source lithology, transport, deposition and sampling scale on the composition of southern California sand. *Sedimentology*, **44**, 653-671.

Critelli S., Marsaglia K.M., and Busby C.J. 2002. Tectonic history of a Jurassic backarc basin sequence (the Gran Cañon Formation) based on compositional modes of tuffaceous deposits. *Geological Society of America Bulletin*, **114**, 515-527.

Critelli S., Le Pera E., Galluzzo F., Milli S., Moscatelli M., Perrotta S. and Santantonio M., 2007. Interpreting siliciclastic-carbonate detrital modes in Foreland Basin Systems: an example from Upper Miocene arenites of the Central Apennines, Italy. In Arribas J., Critelli S. and Johnsson M. (eds), *Sedimentary Provenance: Petrographic and Geochemical Perspectives*. Geological Society of America Special Paper **420**, 107-133.

Critelli, S., Muto, F., Tripodi, V. and Perri, F. 2011. Relationships between lithospheric flexure, thrust tectonics and stratigraphic sequences in foreland setting: the Southern Apennines foreland basin system, Italy: In: Schattner, U., (ed.) *New Frontiers in Tectonic Research at the Midst of Plate Convergence*. Intech Open Access Publisher, Janeza Trdine 9, Rijeka, Croatia, 121-170.

Critelli, S., Muto, F., Perri, F. and Tripodi, V. 2017. Interpreting Provenance Relations from Sandstone Detrital Modes, Southern Italy Foreland Region: stratigraphic record of the Miocene tectonic evolution. *Marine and Petroleum Geology*, **87**, 47-59.

D'Elia, L., Martí, J., Muravchik, M., Bilmes, A. and Franzese J.R. 2018. Impact of volcanism on the sedimentary record of the Neuquén rift basin, Argentina: towards a cause and effect model. *Basin Research*, **30**, 311-335.

Di Capua, A. and Groppelli, G. 2018. The riddle of volcaniclastic sedimentation in ancient deep-water basins: a discussion. *Sedimentary Geology*, **378**, 52-60.

Di Capua, A. and Scasso, R.A., 2020. Sedimentological and petrographic evolution of a fluvio-lacustrine environment during the onset of volcanism: volcanically-induced forcing of sedimentation and environmental responses. *Sedimentology*, **67**, 1879-1913.

Di Capua, A., Barillaro, F. and Groppelli, G., 2021a. Deep-Water Accumulation of Volcaniclastic Detritus from a Petrographic Point of View: Beginning a Discussion from the Alpine Peripheral Basins. *Geosciences*, **11** (441) 1-12,

Di Capua, A., Barillaro, F. and Groppelli, G., 2021b. Volcanism and Volcanogenic Submarine Sedimentation in the Paleogene Foreland Basins of the Alps: Reassessing the Source-to-Sink Systems with an Actualist View. *Geosciences*, **11** (23), 1-21.,

Dickinson, W.R. 1970a. Interpreting detrital modes of graywacke and arkose. *Journal of Sedimentary Petrology*, **40**, 695-707.

Dickinson, W.R. 1970b. Relations of andesites, granites, and derivative sandstones to arc-trench tectonics. *Reviews of Geophysics and Space Physics*, **8**, 813-860.

Dickinson, W.R. 1973. Reconstruction of past arc-trench systems from petrotectonic assemblages in the island arcs of the Western pacific. In: Coleman, P.J. (ed.) *The Western Pacific: Island Arcs, Marginal Seas, Geochemistry*. University of Western Australia Press, 569-601.

Dickinson, W.R. 1976. Plate tectonic evolution of sedimentary basins. *American Association of Petroleum Geologists Continuing Education Course Notes Series* **1**, 62 p.

Dickinson, W.R. 1982. Composition of sandstones in Circum-Pacific subduction complexes and fore-arc basins. *American Association of Petroleum Geologists Bulletin*, **66**, 121-137.

Dickinson, W. R. 1985. Interpreting provenance relations from detrital modes of sandstones. In: Zuffa G.G. (ed.), *Provenance of Arenites*. NATO-ASI Series, Reidel, Dordrecht, 333-361.

Dickinson, W. R. and Suczek, C. A. 1979. Plate tectonics and sandstone compositions. *American Association of Petroleum Geologists Bulletin*, **63**, 2164–2182.

Elter, F.M., Gaggero, L., Mantovani, F., Pandeli, E. and Costamagna, L. 2020. The Atlas-East Variscan-Elbe shear system and its role in the formation of the pull-apart Late Paleozoic basins. *International Journal of Earth Sciences*, **109**,739–760.

Erskine, D.W. and Smith, G.A. 1993. Compositional characterization of volcanic products from a primarily sedimentary record: The Oligocene Espinaso Formation, north-central New Mexico. *Geological Society of America Bulletin*, **105**, 1214-1222.

Fisher, R.V. and Schmincke, H.-U. 1984. *Pyroclastic rocks*. Berlin, Berlin, Springer-Verlag, 472p.

Fisher, R.V. and Smith, G.A. 1991. Volcanism, tectonics and sedimentation. In: Fisher R.V. and Smith G.A. (eds.) *Sedimentation in Volcanic Settings*. *Society of Economic Paleontologists and Mineralogists Special Publication* **45**, 1-5.

Garzanti, E., Critelli, S. and Ingersoll, R.V. 1996. Paleogeographic and paleotectonic evolution of the Himalayan Range as reflected by detrital modes of Tertiary sandstones and modern sands (Indus transect, India and Pakistan). *Geological Society of America Bulletin*, **108**, 631-642.

Garzanti, E., Vezzoli, G., Andò, S. and Castiglioni, G. 2001. Petrology of Rifted-Margin Sand (Red Sea and Gulf of Aden, Yemen). *The Journal of Geology*, **109**, 277-297.

Garzanti, E., Doglioni, C., Vezzoli, G. and Andò, S., 2007. Orogenic belts and orogenic sediment provenances. *The Journal of Geology*, **115**, 315–334.

Gazzi, P., 1966. Le arenarie del flysch sopracretaceo dell'Appenino modenese; correlazioni con il flysch di Monghidoro. *Mineralogica et Petrografica Acta*, **12**, 69–97.

Heiken, G. and Wohletz, K.H. 1985. *Volcanic Ash*. University of California Press, 246 p.

Ingersoll, R.V. 1990. Actualistic sandstone petrofacies: discriminating modern and ancient source rocks. *Geology*, **18**, 733–736.

Ingersoll, R.V., 2001. Structural and stratigraphic evolution of the Rio Grande rift, northern New Mexico and southern Colorado. *International Geology Review*, **43**, 867-891.

Ingersoll, R.V., 2012. Tectonics of sedimentary basins. In: Busby, C.J. and Azor A. (eds.), *Tectonics of Sedimentary Basins. Recent Advances*. Wiley-Blackwell Science, Oxford, 3-43.

Ingersoll, R,V. and Cavazza, W. 1991. Reconstruction of Oligo-Miocene volcaniclastic dispersal patterns in North-Central New Mexico using sandstone petrofacies. In: Fisher R.V. and Smith G.A. (eds.) *Sedimentation in Volcanic Settings*. *Society of Economic Paleontologists and Mineralogists Special Publication* **45**, 225-236.

Ingersoll, R.V., Bullard, T.F., Ford, R.L., Grimm, J.P., Pickle, J.D. and Sares, S.W. 1984. The effect of grain size on detrital modes: a test of the Gazzi-Dickinson point-counting method. *Journal of Sedimentary Petrology*, **54**, 103-116.

Ingersoll, R.V., Kretchmer, A.G. and Valles, P.K. 1993. The effect of sampling scale on actualistic sandstone petrofacies. *Sedimentology*, **40**, 937–953.

Jafarzadeh, M., Shoghani-Motlagh, M., Mousivand, F., Criniti, S. and Critelli, S. 2022. Compositional and Geochemical Signatures of Oligocene copper-bearing sandstones of Abbasabad-Kahak area, NE Iran: Implications for provenance relations and paleogeography. *Marine and Petroleum Geology*, **139**, 1-14 (105605) [https://doi.org/10.1016/j.marpetgeo.2022.105605].

Le Pera, E. and Morrone, C. 2020. The use of mineral interfaces in sand-sized volcanic rock fragments to infer mechanical durability. *Journal of Palaeogeography*, **9**, 1-26.

Le Pera, E., Morrone, C., Arribas J., Arribas M.E., Ancochea E. and Huertas M.J. 2021. Petrography and provenance of beach sands from volcanic oceanic islands: Cabo verde, Atlantic ocean. *Journal of Sedimentary Research*, **91**, 92-115.

Malekzadeh, M., Hosseini-Barzi, M., Sadeghi, A. and Critelli, S. 2020. Geochemistry of Asara Shale member of Karaj Formation, Central Alborz, Iran: Provenance, Source Weathering and Tectonic Setting. *Marine and Petroleum Geology*, **121**, 1-13 (104584) [https://doi.org/10.1016/j.marpetgeo.2020.104584].

Marsaglia, K.M. 1991. Provenance of sands and sandstones from the Gulf of California, a rifted continental arc. In: Fisher R.V. and Smith G.A. (eds.) *Sedimentation in Volcanic*

Settings. *Society of Economic Paleontologists and Mineralogists Special Publication* **45**, 237-248.

Marsaglia, K.M., 1992. Petrography and provenance of volcaniclastic sands recovered fromthe Izu–Bonin arc, Leg 126. *Proceedings of the Ocean Drilling Program, Scientific Results* **126**, 139–154.

Marsaglia, K.M. 1993. Basaltic Island Sand Provenance. In Johnsson, M.J. and Basu, A. (eds.) *Processes controlling the composition of clastic sediments*. *Geological Society of America Special Paper* **284**, 41-65.

Marsaglia, K.M. and Devaney, K.A. 1995. Tectonic and magmatic controls on backarc basin sedimentation: The Mariana region reexamined. In: Taylor, B. (ed.), *Back-arc basins: Tectonics and magmatism*. New York, Plenum Press, 497–520.

Marsaglia, K. M. and Ingersoll, R. V. 1992. Compositional trends in arc-related, deep-marine sand and sandstone: a reassessment of magmatic-arc provenance. *Geological Society of America Bulletin*, **104**, 1637-1649.

Marsaglia, K.M., Ingersoll, R.V. and Packer, B.M. 1992. Tectonic evolution of the Japanese islands as reflected in modal compositions of Cenozoic forearc and backarc sand and sandstone. *Tectonics*, **11**, 1028-1044.

Marsaglia K.M., Barone M., Critelli S., Busby C. and Fackler-Adams B. 2016. Petrography of volcaniclastic rocks in intra-arc volcano-bounded to fault-bounded basins of the Rosario segment of the Lower Cretaceous Alisitos oceanic arc, Baja California, Mexico. *Sedimentary Geology*, **336**, 138-146.

Maynard, J.B., Valloni, R. and Yu, H.-S. 1982. Composition of modern deep-sea sands from arc-related basins. In: Leggett, J.K. (ed.), *Trench-Forearc Geology*. *Geological Society of London, Special Publication*, **10**, 551–561.

McPhie J., Doyle M. and Allen R, 1993. *Volcanic Textures - A Guide to the Interpretation of Textures in Volcanic Rocks*. Hobart, CODES Key Centre, University of Tasmania, 196 p.

Morrone, C., De Rosa, R., Le Pera, E. and Marsaglia, K.M. 2017. Provenance of volcaniclastic beach sand in a magmatic-arc setting: An example from Lipari island (Aeolian archipelago, Tyrrhenian Sea). *Geological Magazine*, **154**, 804-828.

Morrone, C., Le Pera, E., Marsaglia, K.M. and De Rosa, R. 2020. Compositional and textural study of modern beach sands in the active volcanic area of the Campania region (southern Italy). *Sedimentary Geology*, **396**, 1-18.

Morrone, C., Le Pera, E., Marsaglia, K.M., De Rosa, R., 2022. Provenance controls on volcaniclastic beach sand: example from the Aeolian archipelago, Mediterranean SeaIn: Di Capua, A., De Rosa, R., Kereszturi, G., Le Pera, E., Rosi, M. and Watt, S. F. L. (eds), *Volcanic Processes in the Sedimentary Record: When Volcanoes Meet the Environment*. *Geological Society, London, Special Publications*, **520**, 1-34.

Packer, B.M. and Ingersoll, R.V. 1986. Provenance and petrology of Deep Sea Drilling Project sands and sandstones from Japan and Mariana forearc and backarc regions. *Sedimentary Geology*, **51**, 5–28.

Saccani, E. 1987. Double provenance of sand-size sediments in the southern Aegean forearc basin. *Journal of Sedimentary Petrology*, **57**, 736-745.

Smith, G.A., 1991. Facies sequences and geometries in continental volcaniclastic sequences. In: Fisher R.V. and Smith G.A. (eds.) *Sedimentation in Volcanic Settings*. *Society of Economic Paleontologists and Mineralogists Special Publication*, **45**, 109-121.

Smith G.A. and Lotosky, J.E., 1995. What factor control the composition of andesitic sand?. *Journal of Sedimentary Research*, **65**, 91-98.

Sohn, Y.K., Park, K.H. and Yoon, S.-H., 2008. Primary versus secondary and subaerial versus submarine hydrovolcanic deposits in the subsurface of Jeju Island, Korea. *Sedimentology*, **55**, 899-924.

Valloni, R. 1985. Reading provenance from modern marine sands. In: Zuffa G.G. (ed.) *Provenance of Arenites*. NATO-ASI Series, Reidel, Dordrecht, 309–332.

White J.D.L. and Houghton B.F., 2006. Primary volcaniclastic rocks. *Geology*, **34**, 677-680.

Zuffa, G.G. 1980. Hybrid arenites: their composition and classification. *Journal of Sedimentary Petrology*, **50**, 21-27.

Zuffa, G.G. 1985. Optical analysis of arenites: influence of methodology on compositional results. In: Zuffa G.G. (ed.) *Provenance of Arenites*. NATO-ASI Series, Reidel, Dordrecht, 165–190.

Zuffa, G.G. 1987. Unravelling hinterland and offshore paleogeography from deepwater arenites. In: Leggett, J.K. and Zuffa, G.G. (eds) *Deep-Marine Clastic Sedimentology: Concepts and Case Studies*. Graham and Trotman, London, 39–61.

Figure Captions

Fig. 1.- Triangular plots for volcaniclastic sand(stone) suites, illustrating contributions from active volcanic sources. (a) QFL plot (with superposed provenance fields of Dickinson, 1985, and Marsaglia and Ingersoll, 1992) subdividing volcanic contributions in magmatic arc-setting, from intraoceanic+continental and continental active arcs. (b) Lvv (vitric)-Lvmi (microlitic)-Lvl (lathwork) plot. (c) Lvf (felsitic)-Lvmi (microliticc)-Lvl (lathwork). (d) Lvf (felsitic)-Lvv (vitric)-Lvmi+Lvl (microlitic+lathwork). Plots (b), (c), (d) subdivide volcanic contributions in relations to style and composition of active volcanism from mafic, intermediate, and felsic (high silicic) sources. From Dickinson (1970a, 1985), Marsaglia (1991), Marsaglia and Ingersoll (1992), Critelli and Ingersoll (1995), Critelli *et al*. (2002) and Marsaglia *et al*. (2016).

Fig. 2.- (a) Lvg-Lvv-Lvmi+Lvl, (b) Lvvg-Lvs-Lvmi (Affolter and Ingersoll, 2019) triangular plots showing proportions of volcanic glass, aphanitic microlites, and subhedral and euhedral microlites that define volcanic textural types (Lvv, Lvg, Lvs, Lvm, and Lvl). All internal lines are at 5% or 95%. Felsitic (granular) grains with chert-like texture (Lvg)- Felsitic (seriate) grains with irregular mosaics of crystals and glass (Lvs)- Microlitic grains with abundant plagioclase feldspar microlites (Lvmi)- Lathwork grains with plagioclase-and pyroxene laths (Lvl)- Vitric lithic grains defined as glass or altered and commonly showing flow patterns (Lvv). From Affolter and Ingersoll (2019).

Fig. 3.- Photomicrographs of vitric volcanic lithic grains. (a, b) Brown glass is closely related to subaerial or subacqueous volcanism both explosive or lava of mainly intermediate to mafic-volcanic (basaltic to andesitic) eruptions. (c) Orange quenched glass and palagonitic sideromelane glass is closely related to dominantly subaqueous volcanism of mafic-volcanic (basaltic to basaltic andesite) eruptions. (d) Colorless glass, blocky shards; ,(e) bubble-wall shards; and Y-shaped glass (f) closely related to subaerial explosive volcanism of mainly silicic volcanic eruptions. Data set includes volcaniclastic sandstone suites from Jurassic Gran Cañon Formation, Cedros Island, Mexico (A, B), Miocene Topanga Group, Los Angeles Basin, California (C), Miocene Obispo Tuff, Monterey Formation, California (d, e, f). From Critelli and Ingersoll (1995), Critelli et al. (2002). Courtesy of R.F. Fisher and G. Smith for sampling one of us (S. Critelli) the Obispo Tuff (Monterey Formation, California).

Fig. 4.- Photomicrographs of microlitic volcanic lithic grains. (a) Mosaic of plagioclase microlites in black groundmass. (b) Microlites of plagioclase and hornblende minerals that are visible at high magnification. (c-d) Microlitic fragments that contain variable amounts of microlites of plagioclase and rare hornblende that are visible at high magnification. (e) Mosaic of plagioclase microlites in a brown groundmass, typical of basaltic andesite. (f) Mosaic of plagioclase microlites in a black groundmass. Microlitic texture is typical of andesite, but is common in basalts and basaltic andesite. Data set includes volcaniclastic sandstone suites for Cretaceous Alisitos Group, Baja California, Mexico (a, b, c, e, f), and Miocene Topanga Group, Los Angeles Basin, California (d). From Critelli and Ingersoll (1995), and Marsaglia *et al*. (2016).

Fig. 5.- Photomicrographs of lathwork volcanic lithic grains. (a-b) Plagioclase and relict pyroxene in brown glass of basaltic lava flow (a, crossed nicols; b, plane-polarized light). (c-d) Palagonitized brown glass and microlitic groundmass of microlitic plagioclase and pyroxene, and plagioclase and pyroxene laths in basaltic sand(stone) (c, crossed nicols; d, plane-polarized light). (e-f) Euhedral and zoned Ca-rich plagioclase laths in brown palagonitized groundmass of basaltic andesite sand(stone) (e, crossed nicols; f, plane-polarized light). Data set includes volcaniclastic sandstone suites from Jurassic Gran Cañon Formation, Cedros Island, Mexico (A, B, E, F), Miocene Topanga Group, Los Angeles Basin, California (C-D). From Critelli and Ingersoll (1995), and Critelli *et al*. (2002).

Fig. 6.- Photomicrographs of felsitic seriate (a, b, c) and felsitic granular (d, e, f) volcanic lithic grains. (a) Anisometric mosaic, with wide range of crystal sizes and shapes, composed mainly of zoned and twinned plagioclase and green hornblende phenocrysts in vitric groundmass. (b) Anisometric mosaic, composed mainly of feldspar and quartz in microcrystalline groundmass. (c) Anisometric mosaic composed mainly of feldspar, quartz, and hornblende in a vitric or microcrystalline groundmass. Felsitic seriate texture represents mainly silicic-volcanic rocks, either lava or tuff, especially high-K varieties and is typical of andesite and dacite. (d-e) Anhedral microcrystalline mosaics, with uniform very fine grain size, composed mainly of quartz (d) and feldspar (e) representing mainly silicic-volcanic rocks, either lava or tuff. (f) Vitric grains may grade into granular grains through devitrification. Felsitic granular texture is typical of rhyolite, rhyodacite and dacite. Data set includes volcaniclastic sandstone suites for Jurassic Gran Cañon Formation, Cedros Island, Mexico (a, b, c), Cretaceous Alisitos Group, Baja California, Mexico (d), and the Miocene

Topanga Group, Los Angeles Basin, California (e, f). From Critelli and Ingersoll (1995), Critelli *et al*. (2002), and Marsaglia *et al*. (2016).

Fig. 7.- Lvf-Lvv-Lvmi+Lvl triangular plot showing proportions of felsitic (Lvf), volcanic glass (Lvv) and microlitic+lathwork (Lvmi+Lvl), with mean values from other publications for comparison as noted. Data set includes volcaniclastic sandstone suites for Jurassic Gran Cañon Formation, Cedros Island, Mexico; Cretaceous Alisitos Group, Baja California, Mexico; Miocene Topanga Group, Los Angeles Basin, California; Miocene Obispo Tuff, Monterej Formation, California; Cenozoic Rio Grande Rift, New Mexico; Gulf of California; Sumisu Rift; Mariana Rift. Data from: Marsaglia (1991, 1992); Ingersoll and Cavazza (1991); Critelli and Ingersoll (1995), Critelli *et al*. (2002), Marsaglia *et al*. (2016).

Table Captions

Table 1. Optical Analysis of arenites by using Gazzi-Dickinson method (Zuffa, 1980, 1985).

Table 2. Optical Analysis of volcanoarenites by using Gazzi-Dickinson method, distinguishing Paleo-volcanic grains and Neo-volcanic grains (e.g. Zuffa, 1985, 1987; Critelli and Ingersoll, 1995).

Petrographic classes

Quartz (Qt=Qm+Qp)

Quartz (single crystals)

Polycrystalline quartz with tectonic fabric
Polycrystalline quartz without tectonic fabric
Quartz in metamorphic r.f.
Quartz in plutonic r.f.
Quartz in sandstone r.f.
Quartz in plutonic or gneissic r.f.
Calcite replacement on quartz

Feldspars (F=K+P)

K-feldspar (single crystals)
K-feldspar in plutonic r.f.
K-feldspar in sandstone r.f.
Calcite replacement in k-feldspar

Plagioclase (single crystals)

Plagioclase in metamorphic r.f.
Plagioclase in plutonic r.f.
Plagioclase in plutonic or gneissic r.f.
Plagioclase in volcanic r.f.
Plagioclase in sandstone r.f.
Calcite replacement in Plagioclase

Micas

Dense minerals

Dense mineral (single crystal)

Dense mineral in plutonic r.f.
Dense mineral in metamorphic r.f.
Opaque minerals

Extrabasinal Carbonates (CE)

Dolostone
Micritic Limestone
Sparitic Limestone
Microsparitic Limestone
Biomicritic Limestone
Biosparitic Limestone
Fossil (single skeleton)
Fossil in Limestone-Dolostone
Single spar (calcite)
Single spar (dolomite)

Intrabasinal Carbonates (CI) and noncarbonates (NCI)

Bioclast
Peloids
Glauconite
Rip-Up clasts

Interstitial components (Matrix and cements)

Siliciclastic matrix

Micas and chlorite (single crystals)	Carbonate matrix (micrite)
Micas in plutonic r.f.	Carbonate cement (pore-filling)
Micas in metamorphic r.f.	Carbonate cement (patchy calcite)
Lithic fragments (L=Lm+Lv+Ls)	Calcite replacement on underterm. grain
Volcanic lithic with microlithic fabric	Siliceous cement
Volcanic lithic with felsitic granular texture	Phyllosilicate cement
Volcanic lithic with felsitic seriate texture	Oxid-Fe cement
Volcanic lithic with lathwork texture	Alterites (indeterm.alterite grain)
Volcanic lithic with vitric texture	
Serpentinite	
Serpentine-schist	
Phyllite	
Fine-grained Schist	
Fine-grained Gneiss	
Siltstone	
Impure Chert	
Shale	

Table 1

Petrographic classes

PALEOVOLCANIC GRAINS

Quartz

Quartz (single crystals)
Polycrystalline quartz with tectonic fabric
Polycrystalline quartz without tectonic fabric
Quartz in paleovolcanic r.f.
Quartz in other r.f.
Calcite replacement on paleovolcanic quartz

Feldspars

K-feldspar (single crystals)
K-feldspar in paleovolcanic r.f.
K-feldspar in other r.f.
Calcite replacement on paleovolcanic k-feldspar

Plagioclase (single crystals)
Plagioclase in paleovolcanic r.f.
Plagioclase in other r.f.
Calcite replacement on paleovolcanic Plagioclase

Micas

Micas and chlorite (single crystals)
Micas and chlorite in paleovolcanic r.f.
Micas in other r.f.

Lithic fragments

Paleovolcanic lithic with microlithic fabric
Paleovolcanic lithic with felsitic granular texture

NEOVOLCANIC GRAINS

Quartz

Quartz (single crystals)
Polycrystalline quartz without tectonic fabric
Quartz in Volcanic lithic with felsitic granular fabric r.f.
Volcanic lithic with felsitic seriate fabric r.f.

Feldspars

K-feldspar (single crystals)
K-feldspar in felsitic seriate r.f.
K-feldspar in felsitic granular r.f.

Plagioclase (single crystals)
Ca-rich Plagioclase in Volcanic lithic with lathwork fabric r.f.
Ca-rich Plagioclase in Volcanic lithic with microlithic fabric r.f.
Ca-rich Plagioclase in Volcanic lithic with felsitic seriate fabric r.f.
Na-rich Plagioclase in Volcanic lithic with felsitic granular fabric r.f.
Na-rich Plagioclase in Volcanic lithic with felsitic seriate fabric r.f.

Micas

Micas and chlorite (single crystals)
Micas in Volcanic lithic with felsitic granular fabric r.f.
Micas in Volcanic lithic with felsitic seriate fabric r.f.

Lithic fragments

Volcanic lithic with microlithic fabric in black groundmass
Volcanic lithic with microlithic fabric in brown groundmass
Volcanic lithic with microlithic fabric in silicic recrystallized groundmass

Paleovolcanic lithic with felsitic seriate texture
Paleovolcanic lithic with lathwork texture
Paleovolcanic lithic with vitric texture
Other aphanitic lithic grains

Dense minerals

Dense mineral (single crystal)
Dense mineral in paleovolcanic r.f.
Dense mineral in other r.f.
Opaque minerals

Interstitial components (Matrix and cements)

Siliciclastic matrix
Fine-ash volcaniclastic matrix
Carbonate matrix (micrite)
Carbonate cement (pore-filling)
Carbonate cement (patchy calcite)
Calcite replacement on underterm. grain
Siliceous cement
Phyllosilicate cement
Oxid-Fe cement
Alterites (indeterm.alterite grain)

Volcanic lithic with felsitic granular texture
Volcanic lithic with felsitic seriate texture
Volcanic lithic with lathwork texture in black groundmass
Volcanic lithic with lathwork texture in brown groundmass
Volcanic lithic with lathwork texture in orange groundmass
Volcanic lithic with vitric texture black in colour
Volcanic lithic with vitric texture brown-orange in colour (Sideromelane)
Volcanic lithic with colorless vitric texture: blocky shard
Volcanic lithic with colorless vitric texture: bubble-wall shard
Volcanic lithic with vitric texture: scoria fragment
Volcanic lithic with vitric texture: pumice fragment
Volcanic lithic with altered (clay and zeolite) vitric texture

Dense minerals

Dense mineral (single crystal):
Clinopyroxene
Olivine
Hornblende
Others single dense minerals
Opaque minerals
Dense minerals in Volcanic lithic with microlithic fabric
Dense minerals in Volcanic lithic with lathwork fabric
Dense minerals in Volcanic lithic with felsitic seriate fabric
Dense minerals in Volcanic lithic with felsitic granular fabric

Table 2

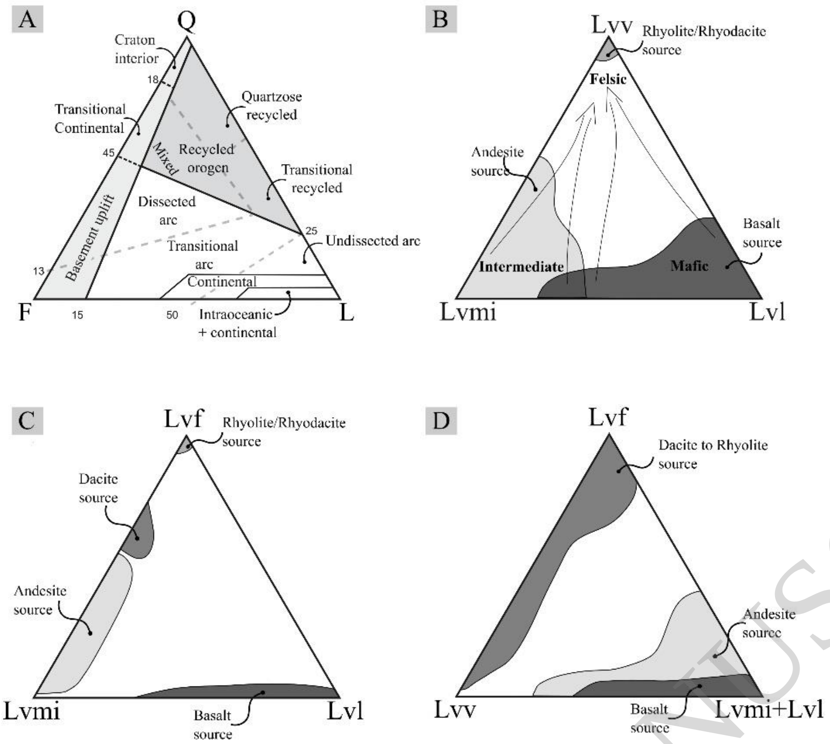
A
Q
Craton interior
18
Transitional Continental
Quartzose recycled
45
Mixed
Recycled orogen
Transitional recycled
Dissected arc
Basement uplift
25
Undissected arc
Transitional arc
13
Continental
F
15
50
Intraoceanic + continental
L
B
Lvv
Rhyolite/Rhyodacite source
Felsic
Andesite source
Basalt source
Intermediate
Mafic
Lvmi
Lvl
C
Lvf
Rhyolite/Rhyodacite source
Dacite source
Andesite source
Lvmi
Basalt source
Lvl
D
Lvf
Dacite to Rhyolite source
Andesite source
Lvv
Basalt source
Lvmi+Lvl

Figure 1

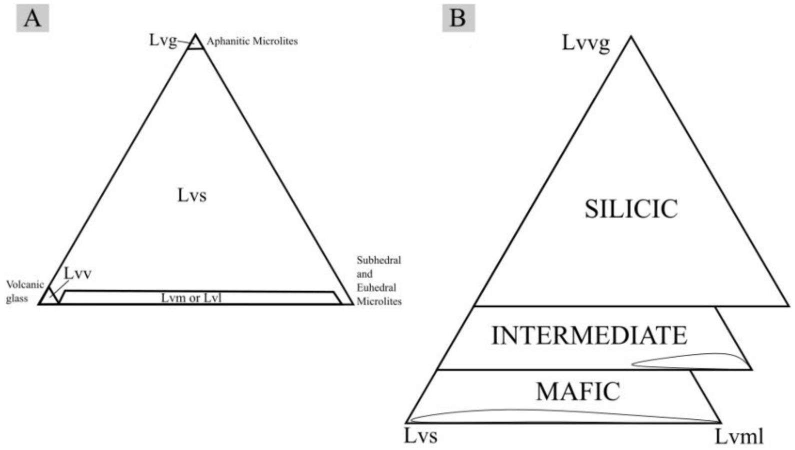
A
Lvg
Aphanitic Microlites
Lvs
Lvv
Volcanic glass
Lvm or Lvl
Subhedral and Euhedral Microlites
B
Lvvg
SILICIC
INTERMEDIATE
MAFIC
Lvs
Lvml

Figure 2

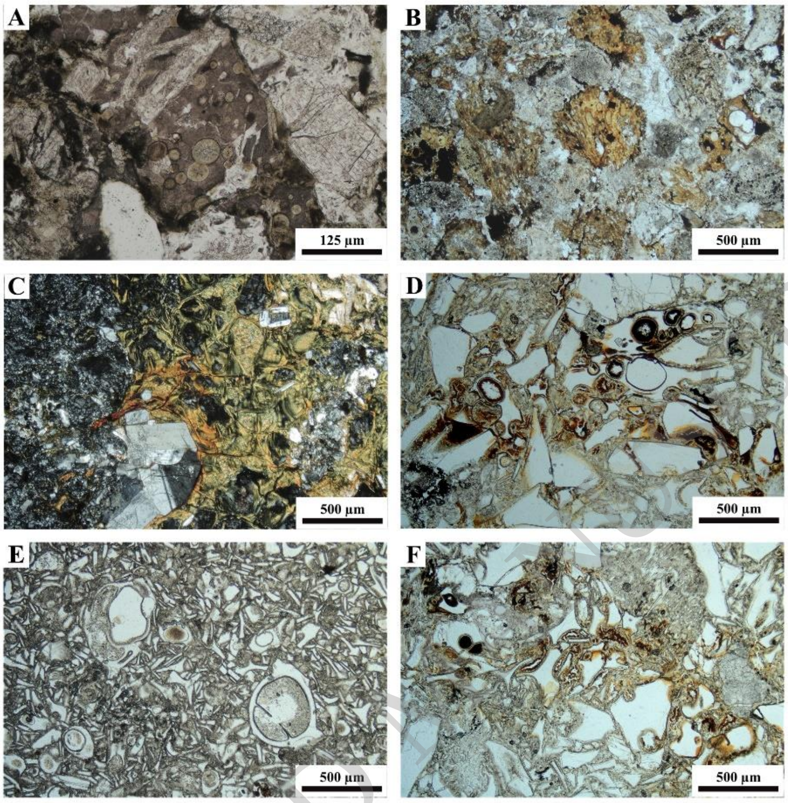

Figure 3

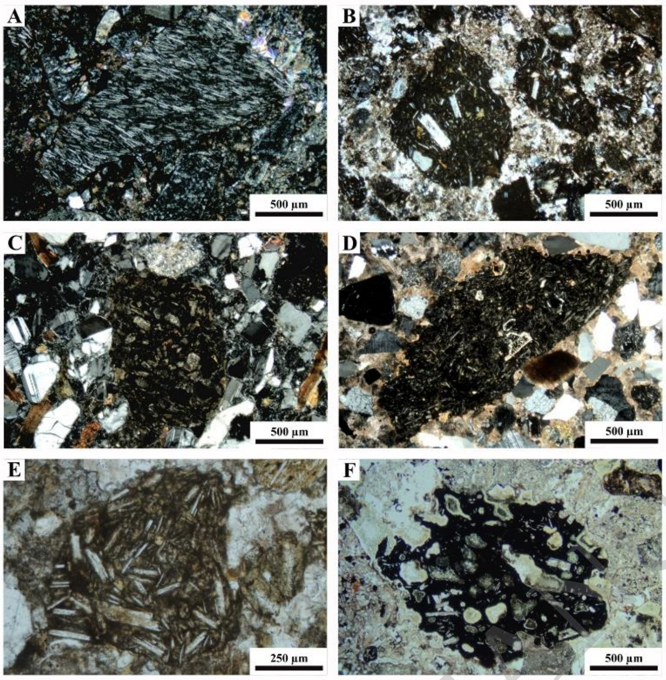

Figure 4

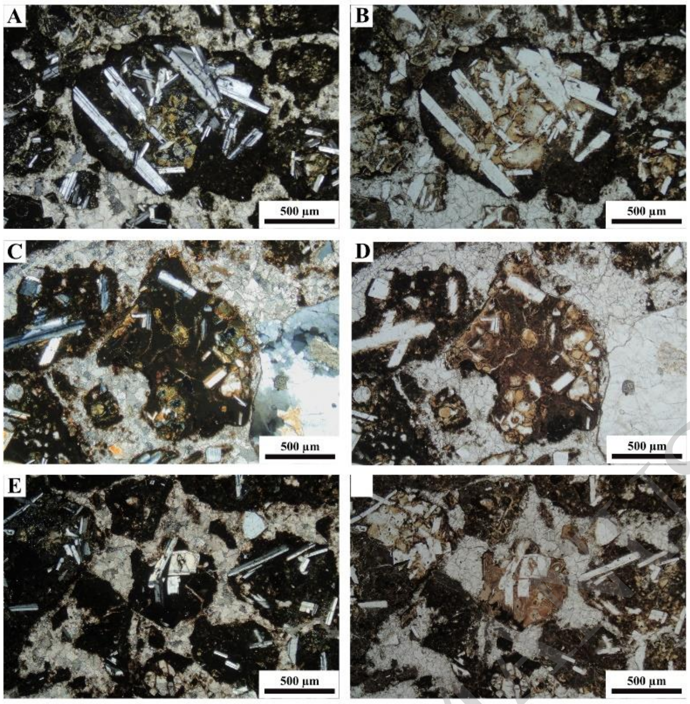

Figure 5

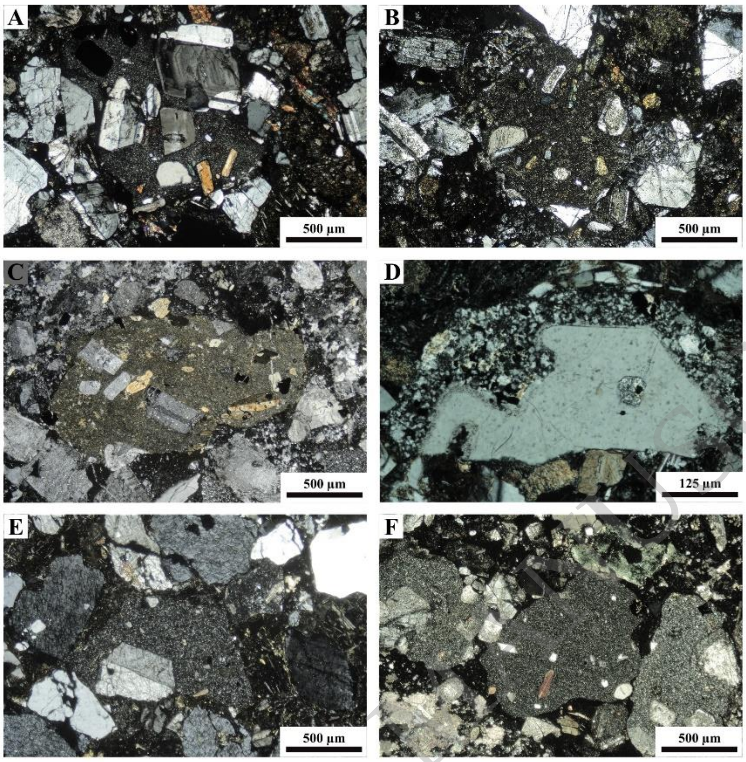

Figure 6

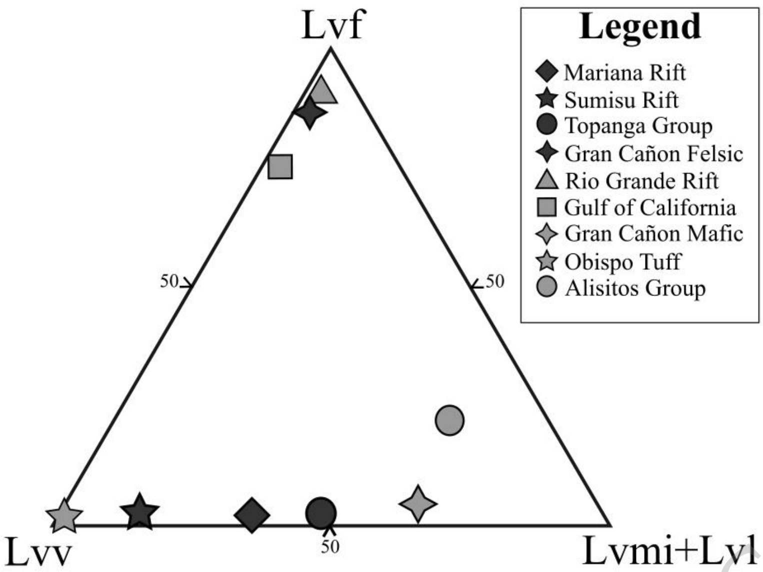
Lvf
Legend
Mariana Rift
Sumisu Rift
Topanga Group
Gran Cañon Felsic
Rio Grande Rift
Gulf of California
Gran Cañon Mafic
Obispo Tuff
Alisitos Group
50
50
50
Lvv
Lvmi+Lvl

Figure 7